Scanning Electrochemical Microscopy. 45. Study of the Kinetics of Oxygen Reduction on Platinum with Potential Programming of the Tip

Biao Liu and Allen J. Bard*

Department of Chemistry and Biochemistry, The University of Texas at Austin, Austin, Texas 78712

Received: August 23, 2002; In Final Form: October 10, 2002

Scanning electrochemical microscopy (SECM) was used to study the kinetics of oxygen reduction on platinum in alkaline media. Oxygen was generated at a gold tip by oxidation of OH^- and reduced at a Pt substrate. The formation of anodic film on the surface of the gold tip caused instability in tip behavior. This problem was overcome by applying a potential program at the tip to obtain the stable steady state tip current that is important for quantitative SECM analysis. The Tafel slope (125 mV, corresponding to a transfer coefficient, α, of 0.47) and the rate constant for oxygen reduction obtained by fitting the approach curves (2×10^{-3} cm s^{-1} at the open circuit potential) agree with previous results obtained by the rotating ring disk electrode technique and other electrochemical methods.

1. Introduction

Electrochemical reduction of molecular oxygen has been the subject of extensive investigations over the last century. This is largely because the O_2 reduction reaction is of major importance to energy conversion, particularly in the field of fuel cells and metal−air batteries.[1−4] After decades of painstaking efforts, many fundamental and practical research findings have been obtained, which are very useful for understanding the general aspects of the O_2 reduction reaction. However, the overall progress in this field has been slow. There is still a large degree of uncertainty regarding the mechanism and intermediates of the O_2 reduction reaction. Most importantly, a low cost and efficient electrocatalyst for O_2 reduction, which would have wide application in fuel cells, metal−air batteries, and many other electrochemical applications, has not yet been discovered. The pronounced irreversibility of the cathodic reaction in aqueous solutions on most metal electrodes and the large number of possible pathways for O_2 reduction make the study of O_2 reduction challenging. The situation is made more complicated by the sensitivity of O_2 reduction rate to the state of the electrode surface. Usually, metal electrodes are covered with an anodic oxide film at the potentials of interest for O_2 reduction and for O_2 evolution.[5,6]

In this paper, scanning electrochemical microscopy (SECM) was used to study oxygen reduction on platinum in alkaline media. SECM allows one to probe local chemical properties of substrate surfaces and examine small structures and has the advantage that kinetic measurements, even of fast reactions, can be made under steady state conditions.[7,8] We and Hillier and co-workers previously used the feedback to the tip electrode to study the fast kinetics of hydrogen oxidation on Pt.[9] The quantitative O_2 reduction rate on Pt was determined from the SECM approach curves. The drift in tip current due to the formation of anodic film was alleviated by applying a periodic potential program to the tip.

In SECM, an ultramicroelectrode, called the tip, is scanned toward and over the surface of a substrate. A plot of the tip current, i_T, as a function of distance between tip and substrate, d, is called an approach curve. The effect of substrate potential
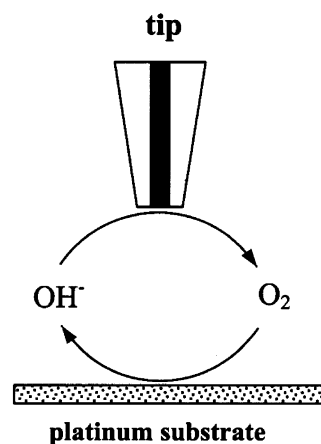
Figure 1. Feedback mode of SECM used in the study of O_2 reduction in alkaline solution.

on i_T can be used to obtain information about the heterogeneous kinetics on the substrate. Topographic images and maps of chemical reactivity across the substrate can also be obtained. The steady state kinetic measurements with SECM are essentially free from complications caused by ohmic drop in solution and double layer charging current that are frequently associated with other electrochemical techniques.[7,8]

Figure 1 illustrates the basic principle of the feedback mode of SECM used in the present work. Hydroxide ion is oxidized at the tip, and the tip potential is adjusted to oxidize OH^- at a diffusion-controlled rate. When the tip is far away from the substrate, a steady state current, $i_{T,\infty}$, flows. This current results from the hemispherical diffusion of OH^- to the tip. As the tip is brought close to the substrate, i.e., within a few tip radii, the O_2 generated at the tip diffuses to the substrate where it can be reduced. This process generates OH^- at the substrate and produces an enhancement in the faradic current at the tip electrode depending on the tip/substrate separation and the rate of reaction at the substrate. Quantitative theory has been developed for different modes of the SECM operation,[7,8] and kinetic parameters of O_2 reduction can be extracted by fitting experimental tip current vs distance (approach) curves to theory.

12802 *J. Phys. Chem. B, Vol. 106, No. 49, 2002*

Liu and Bard
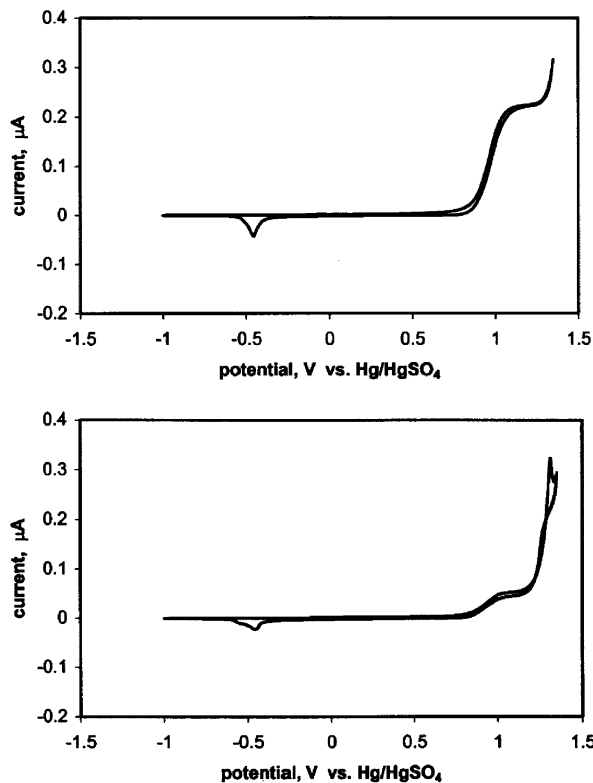
Figure 2. CVs for a 10 mM deaerated solution of sodium hydroxide, recorded with a freshly polished gold disk electrode of 25 μm diameter (a) or with the same electrode that was polarized at 1.2 V for 5 min (b). The solution contained 0.1 M Na_2SO_4. The scan rate was 100 mV/s.

2. Experimental Section

2.1. Chemicals. All chemicals were reagent grade and were used as received. All solutions were prepared with deionized water (Milli-Q, Millipore Corp.).

2.2. Electrodes. Gold or platinum wire (25 μm diameter; Goodfellow, Cambridge, U.K.) was used to construct the tip ultramicroelectrodes for SECM measurements. The procedure of tip preparation has been described elsewhere.[7,8] For tips used here, RG was 3−4. The substrate Pt disk electrode had a diameter of 2.2 mm. The tip and substrate were polished with 0.05 μm alumina and then sonicated with water before use. All potentials given in this paper are referred to the mercury−mercurous sulfate reference electrode (0.64 V vs NHE). A platinum wire was used as the auxiliary electrode.

2.3. Electrochemical Measurements. A CHI 900 SECM (CH Instruments, Austin, TX) was used for all experiments. Cyclic voltammetry experiments were performed in a 10 mL glass vial. SECM experiments were performed in a Teflon cell (∼3 mL). The solution was deaerated with argon. Before each approach curve was recorded, the potential of the Pt substrate electrode was cycled between 0 and −1.3 V until reproducible cyclic voltammograms (CVs) were obtained. The approach curves were obtained by setting the tip potential at 1.2 V (i.e., at the diffusion-limiting current for OH$^-$ oxidation). All of the experiments were carried out at room temperature.

3. Results and Discussion

3.1. Voltammetry of Hydroxide Ion on Gold and Platinum Microelectrodes. Figure 2a shows a typical CV for a deaerated solution of 10 mM sodium hydroxide, recorded with a gold disk electrode of 25 μm diameter. A well-defined sigmoidal wave
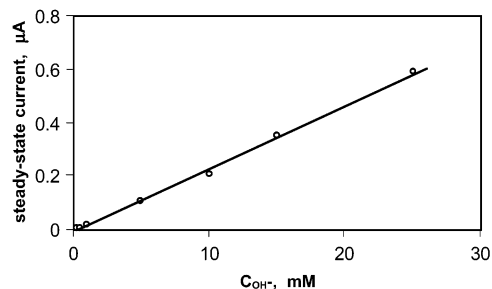
Figure 3. Steady state limiting current vs concentration of sodium hydroxide in aqueous solution containing 0.1 M Na_2SO_4.
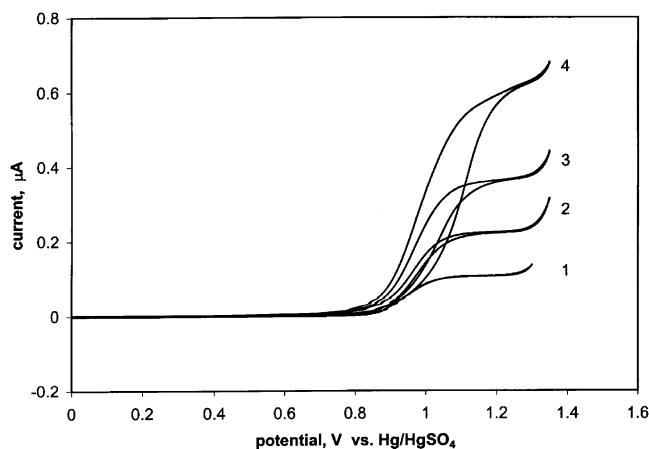

Figure 4. Voltammograms for hydroxide ion oxidation on a 25 μm diameter Au microelectrode in 0.1 M Na_2SO_4 solution. The scan rate was 100 mV/s. The concentration of hydroxide ion: (1) 5, (2) 10, (3) 15, and (4) 25 mM.

for the oxidation to O_2, which occurs before the oxidation of water, was observed at around 1 V, consistent with previous studies of the voltammetry of hydroxide ion in aqueous solutions on gold microelectrodes.[10−12] At potentials more positive than 1.3 V, the current increases significantly due to direct electrochemical oxidation of water. The small oxidation wave observed at ∼−0.2 V and the associated reduction peak at about −0.5 V arise from surface oxide formation and reduction of Au.[5,6,10]

The hydroxide oxidation process showed a diffusion-controlled limiting current that varied directly with the radius of the microelectrode and the concentration of hydroxide ion (eq 1).[10−12] The steady state limiting current at 1.2 V was proportional to the concentration of hydroxide ion over the range of 0.2−25 mM (Figure 3). The limiting current fit the microdisk electrode equation under steady state conditions

$$i_{T,\infty} = 4nFDca \tag{1}$$

where n is the electron transfer number, F is the Faraday constant, D is the diffusion coefficient, c is the concentration of the reactant, and a is the radius of the microdisk. $D = 5.23 \times 10^{-5}$ cm^2/s[13] yields n for the oxidation of OH$^-$ of essentially 1, in accord with the following reaction scheme:

$$4OH^- = O_2 + 2H_2O + 4e^- \tag{2}$$
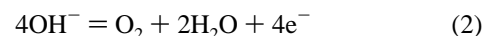
A well-defined CV, with the reverse scan retracing the forward scan, could only be obtained at concentrations of OH$^-$ below about 10 mM. As is evident from Figure 4, hysteresis of the CV wave becomes significant when the concentration of hydroxide ion is as high as 15 mM. This is probably due to formation of O_2 bubbles on the gold surface at higher OH$^-$ concentration. The oxidation wave splits at higher OH$^-$

Oxygen Reduction on Platinum

J. Phys. Chem. B, Vol. 106, No. 49, 2002 **12803**
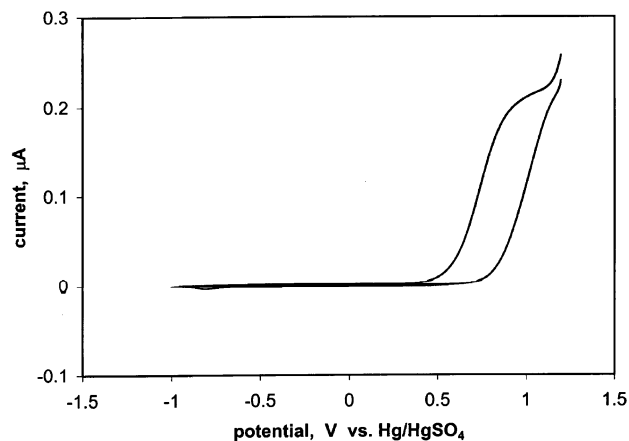
Figure 5. CV recorded with a platinum microelectrode of 25 μm diameter in a solution of 10 mM sodium hydroxide and 0.1 M Na_2SO_4 at 100 mV/s.

concentration.[10] The splitting depends on the dimension of the electrode employed. For example, the splitting occurs on a gold electrode of 25 μm diameter when OH^- concentration is higher than 10 mM.[10] A very small prewave, which is not evident from Figure 4, was observed in the concentration range investigated. The mechanism of splitting is not clear but may be related to the adsorption of OH^- on the gold surface.

Similar CV waves for OH^- oxidation were also observed on a platinum ultramicroelectrode (Figure 5). At the given concentration of OH^-, the oxidation wave appeared at a less positive potential on Pt than on Au (as compared to Figure 2), but the current plateau corresponding to OH^- oxidation was less well-defined on Pt because the water oxidation also occurred at less positive potentials.[14] Because the wave due to OH^- oxidation was less defined on Pt than on Au, only the latter was used in the SECM measurements.

3.2. Effect of Oxide Formation on Steady State Current for Hydroxide Oxidation on the Au Tip. As shown in Figure 2, oxygen evolution from OH^- on Au occurs in the potential region where surface oxides are formed. Thus, at the tip potential where OH^- is oxidized at a diffusion-controlled rate ($\sim$1.2 V), the tip current ($i_{T,\infty}$) corresponds to two processes that occur concurrently, namely, the oxidation of OH^- and the transient current due to formation of the surface oxides:

$$i_{T,\infty} = i_{T,\infty,OH^-} + i_{T,\infty,oxide} \quad (3)$$

The development of Au oxide in alkaline solution has been proposed to proceed through the following stages:[5]

$$Au + OH^- - e^- \rightarrow AuOH \rightarrow AuO \quad (4)$$

At more positive potentials and after long periods of oxidation, Au in the 3+ oxidation state (e.g., Au_2O_3) may be formed.[5,14] Studies of surface oxidation of noble metal electrodes have revealed that the extent of oxidation depends on the potential, oxidation time, and temperature.[4−6] The longer the oxidation time, the greater the magnitude of the metal oxidation. At a constant positive potential, the anodic current decreases exponentially with an increase in the surface oxide coverage or oxide thickness on the electrode.[4]

Oxide formation on a noble metal markedly influences the mechanism and kinetics of various anodic processes occurring on the electrode surface. After the oxides are formed, the electronic properties of the metal surface and the adsorption behavior of reaction intermediates and products at the electrode surface will be changed. The oxide can also impose a barrier to
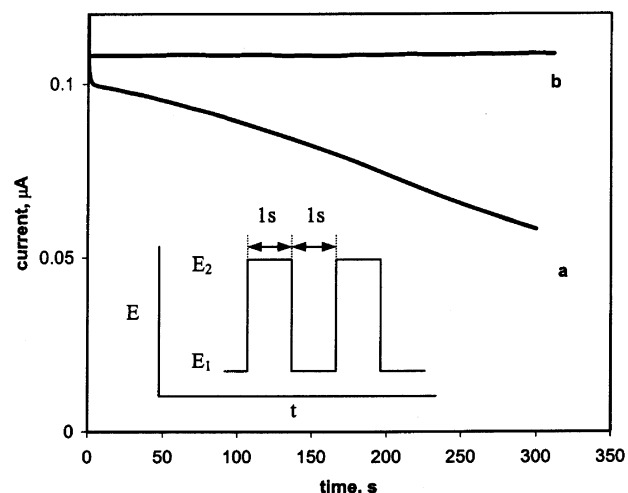
Figure 6. Plot of limiting current against time for a 12.5 μm radius Au microelectrode held at a constant potential (1.2 V) (a) and with a programmed potential (b). The solution was 5 mM in sodium hydroxide and 0.1 M in Na_2SO_4. The inset shows the potential profiles for (b). E_1 was −0.9 V, and E_2 was 1.2 V.

charge transfer at the electrode/electrolyte interface. Accordingly, the rate of OH^- oxidation at the Au surface will be influenced by the growth of surface oxides. This continuous oxide build up on Au or Pt will change the value of the limiting current $i_{T,\infty}$ by altering both i_{T,∞,OH^-} and $i_{T,\infty,oxide}$. The unstable limiting current makes quantitative SECM analysis difficult. This aspect was investigated on an Au microelectrode in NaOH solution. After a constant potential was applied to a freshly polished Au microelectrode so that OH^- was oxidized at a diffusion-controlled rate, $i_{T,\infty}$ decayed (Figure 6a). The decrease in the reactivity of OH^- oxidation caused by surface oxide was also observed in the CV shown in Figure 2b, which was recorded immediately after a 5 min anodic polarization. As compared to the CV for freshly polished Au (Figure 2a), the oxidation current for OH^- oxidation on the oxide-covered Au surface was dramatically decreased, perhaps because the reaction rate was no longer diffusion-controlled. While the exact mechanism for this decrease was not studied further, its effect on the tip current compromises SECM measurements. Note that the rate of water discharge on the oxide-covered surface appeared to increase because convection gives rise to current oscillation over the same potential range, caused by O_2 bubbles forming on the electrode surface.

To obtain a stable $i_{T,\infty}$, a potential program was applied to the Au tip so that any oxide produced during anodic polarization was reduced before the anodic OH^- oxidation measurement. Such potential programming has been frequently used in the past to obtain reproducible surface conditions on solid electrodes.[15] The potential waveform applied is shown in the inset of Figure 6, where the potential was stepped to −0.9 V for 1 s followed by a step to 1.2 V for the measurement. The tip current was always measured at the end of the pulse at 1.2 V. As shown in Figure 6b, this potential programming approach led to a stable limiting current (within 5% over 30 min continuous cycling) indicating reproducible regeneration of the electrode surface. Such a programmed tip potential approach in SECM could also be used to clean the electrode surface after adsorption of blocking impurities at low concentration in solution. Recently, Abdelsalam et al. exploited the steady state voltammetry of OH^- on Au microelectrodes in a study of the detection of OH^- in aqueous solution.[10] A similar potential modulation was employed to obtain a reproducible limiting current in these studies. The reproducibility of the steady state limiting current of OH^-
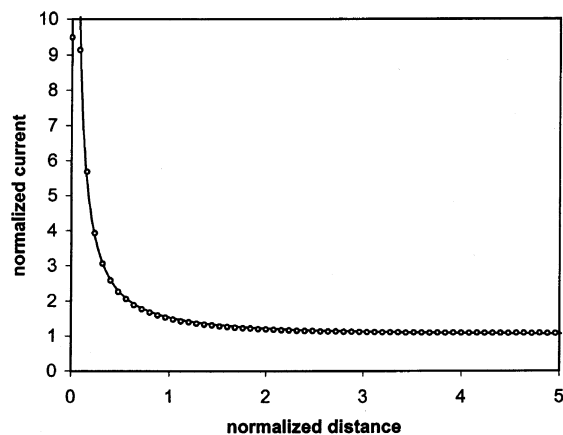
Figure 7. SECM approach curve obtained on a platinum substrate with the tip potential modulated. The tip potential profiles are the same as that shown in the inset of Figure 6 (here, the lowest potential E_1 and highest potential E_2 were -0.1 and 0.35 V, respectively). The tip was a 12.5 μm radius Au microdisk. The aqueous solution was 1 mM in ferrocenemethanol and 0.1 M in KCl. Approach speed was 0.5 μm/s. The solid line is a theoretical approach curve at a conducting substrate.

oxidation is particularly important for the analytical applications and in obtaining usable approach curves in SECM.

In previous SECM measurements, a constant potential was applied to the working tip to obtain approach curves.[7,8] To check the applicability of the programmed tip potential mode in SECM measurements, ferrocenemethanol was used as a mediator to obtain the approach curve by applying 1 s potential steps between 0.35 and -0.1 V to the Au tip. Figure 7 shows the approach curve obtained for ferrocenemethanol on a conductive substrate. The experimental curve fit theoretical curve quite well, indicating that the potential program mode is indeed useful in obtaining approach curves. Note that the tip current under this potential programmed approach will not be identical to the true steady state current, depending upon tip radius and diffusion coefficient of mediator, because the transient part of the current may not have completely died away within the 1 s step. That is, the required condition $a^2/D \ll 1$ s may not be fully met. In practice, we found the current under programmed conditions to be within 3% of the steady state current. Longer potential steps could be used, but this would decrease the data density or increase the time needed to scan an approach curve.

3.3. Oxygen Reduction on Pt. As stated in the preceding section, SECM can be used to measure the rate constants for heterogeneous electron transfer on substrates by fitting the approach curve. The fitting is based on the SECM theory for a process governed by finite substrate heterogeneous kinetics.[16−18] According to the theory, the following equations can be used to extract the first-order effective heterogeneous electron transfer rate constant:

$$I_T^k = I_S^k (1 - I_T^{ins}/I_T^c) + I_T^{ins} \quad (5)$$

$$I_S^k = 0.78377/L(1 + 1/\Lambda) + [0.68 + 0.3315 \exp(-1.0672/L)]/[1 + F(L, \Lambda)] \quad (6)$$

where I_T^c, I_T^k, and I_T^{ins} represent the normalized tip currents for diffusion-controlled regeneration of redox mediator, finite substrate kinetics, and insulating substrate (i.e., no mediator regeneration), respectively, at a normalized tip−substrate separation, $L = d/a$; I_S^k is the kinetically controlled substrate current; $\Lambda = kd/D$, where k is the apparent heterogeneous rate constant (cm/s), and $F(L, \Lambda) = (11 + 2.3\Lambda)/[\Lambda(110 - 40L)]$.
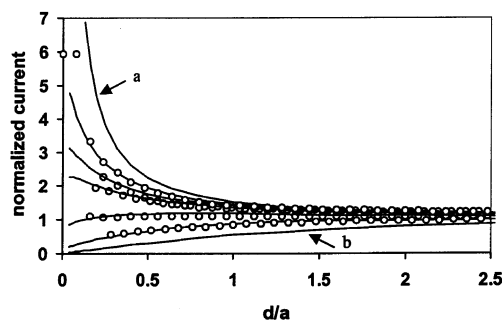
Figure 8. SECM approach curves. The solid lines a and b are theoretical approach curves at conducting and insulating substrates, respectively. Circle symbols are experimental approach curves, and solid lines are theoretical curves at a Pt substrate with its potential held at, from top to bottom, -0.9, -0.8, -0.7, -0.6, and -0.5 V. Approach speed was 0.45 μm/s. The tip was a 12.5 μm radius Au microdisk. The solution contained 10 mM sodium hydroxide and 0.1 M in Na$_2$-SO$_4$. The two highest experimental points occurred with the -0.9 V scan when the tip touched the substrate and were not used in the curve fitting.
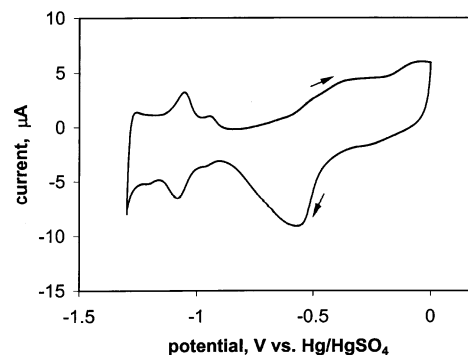
Figure 9. CV recorded with a platinum disk of 2.2 mm diameter in a deaerated solution of 10 mM sodium hydroxide and 0.1 M Na$_2$SO$_4$ at 100 mV/s.

These currents are normalized by the tip current at an infinite tip−substrate separation, $i_{T,\infty}$. The analytical approximations for I_T^c and I_T^{ins}

$$I_T^c = 0.78377/L + 0.3315 \exp(-1.0672/L) + 0.68 \quad (7)$$

$$I_T^{ins} = 1/(0.15 + 1.5358/L + 0.58 \exp(-1.14/L) + 0.0908 \exp[(L - 6.3)/(1.017L)]) \quad (8)$$

have been derived previously.[19]

To measure the O$_2$ reduction rate on platinum, approach curves were obtained by the above potential program that sets the potential of the Au tip to a value where diffusion-controlled oxygen evolution occurs at the tip and moves the tip toward the Pt substrate, held at different potentials. Figure 8 shows approach curves at different substrate potentials as well as theoretical curves for a diffusion-controlled reaction and no reaction at the substrate. Before approaching the tip to the substrate, the substrate potential was cycled between 0 and about -1.3 V several times until reproducible substrate CV waves were observed (Figure 9). The rate constant for the heterogeneous reduction of oxygen on Pt was obtained by fitting the approach curves to the theoretical ones (Figure 10). The diffusion coefficient of hydroxide ion was determined using the data shown in Figure 3 according to eq 1, assuming $n = 1$. A value of 4.89×10^{-5} cm^2/s was obtained, which was used for the curve fitting. The diffusion coefficient of oxygen was assumed to be the same for the purposes of the curve fitting. In

Oxygen Reduction on Platinum

J. Phys. Chem. B, Vol. 106, No. 49, 2002 **12805**
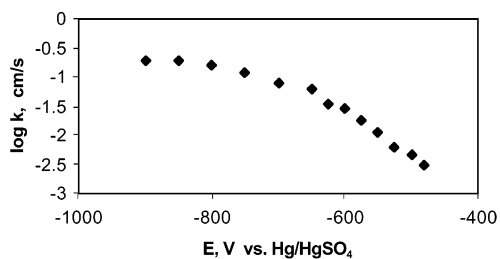
Figure 10. Heterogeneous reaction rate constant k of O_2 reduction at a Pt substrate with different potentials. k was obtained by fitting the experimental approach curves with the theoretical ones as shown in Figure 8.
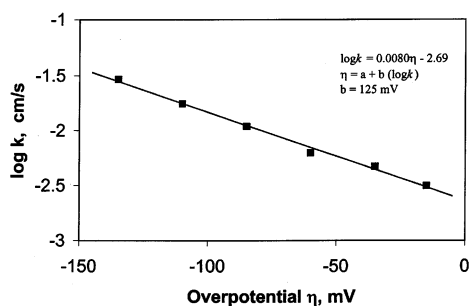
Figure 11. Tafel plot of O_2 reduction on platinum.

actuality, it is slightly different (2.5×10^{-5} cm^2/s in 0.1 M Na$_2$SO$_4$[20]); this small difference will not significantly affect the determined rate constants.

When the substrate potential was more positive than -0.4 V, the oxygen reduction rate was so slow that the approach curves were almost identical to those obtained on an insulator surface. This potential corresponds to the start of Pt oxide formation (Figure 9) at around -0.4 V, which is close to previously reported values.[21] The rate of oxygen reduction on Pt is known to decrease with increasing oxide coverage.[22,23] Thus, the slow O_2 reduction rate at potential beyond -0.4 V can be attributed to low catalytic activity on the oxide-covered surface.

Between -0.45 and -0.6 V, the O_2 reduction rate increased with a decrease of substrate potential. Figure 11 is a plot of the O_2 reduction rate from the approach curves vs overpotential (equivalent to a Tafel plot). The open circuit potential (-0.46 V) was taken as the equilibrium potential E_{eq} in order to calculate the overpotential. Over this potential range, the Tafel plot was a straight line, with a slope of 125 mV, close to a typical Tafel slope of 118 mV.[24] The slope corresponds to a transfer coefficient, α, of 0.47. A 120 mV Tafel slope for O_2 reduction on Pt in alkaline solutions was obtained by different researchers over the same potential range using the rotating ring disk electrode technique.[1-4] Various mechanisms for O_2 reduction on Pt have been proposed. Most of these involve the adsorption of O_2 on the metal surface followed by two or more charge transfer steps.[25] The 120 mV Tafel slope implies that the first charge transfer step is likely to be the rate-determining step.[1-4]

By extrapolating the line in the Tafel plot to $E = E_{eq}$, a rate constant k of 2×10^{-3} cm s^{-1} was obtained. The order of magnitude of the rate constant agrees with the data obtained using rotating ring disk electrode technique and other conventional electrochemical techniques.[1,22,24]

When the substrate potential was more negative than -0.8 V, the rate constant reached a limiting value (Figure 10). This limiting current is not due to mass transfer control, which under these conditions, from previous experience, would be at a value

above 1 cm/s, so that in this potential range the rate-determining step is likely to be a chemical process prior to the electron transfer step, say, the dissociative adsorption of O_2 molecules.

As is evident from Figure 9, hydrogen adsorption and the discharge of water started as the substrate potential became more negative than -0.9 V, which results in a change in the concentration of OH$^-$ at the substrate surface. Furthermore, increasing coverage by chemisorbed hydrogen formed during the discharge of water molecules inhibits the reduction of O_2 on platinum.[4] For these reasons, SECM measurements were not attempted beyond a potential of -0.9 V.

4. Conclusions

The feedback mode of SECM was used to study the kinetics of oxygen reduction on platinum in alkaline media. A gold ultramicroelectrode, on which a well-defined oxidation wave of OH$^-$ was obtained, was used as the SECM tip. A surface oxide formed on the gold tip in the potential range where the oxidation of OH$^-$ occurs, which caused decay of the steady state tip current. By applying a potential program to the gold tip electrode consisting of consecutive stepped potentials to reduce oxide and then oxidize OH$^-$, a stable steady state tip current was obtained, enabling quantitative SECM measurements. This potential programming of the SECM tip should be useful in many circumstances where tip fouling is a problem.

SECM approach curves were then used to study oxygen reduction on a Pt substrate. The Tafel slope and the rate constant for O_2 reduction on platinum obtained with SECM agreed with the data obtained using a rotating ring disk electrode and other electrochemical techniques. These studies demonstrate that SECM is useful in the evaluation of the activity of a catalyst surface for O_2 reduction. The scanning capability of SECM will be particularly useful for this purpose because the distribution of the catalytic activity over a substrate surface can be probed. Moreover, this approach should be useful in applying SECM in combinatorial studies of oxygen reduction catalyst activities.[26]

References and Notes

(1) Markovic, N. M.; Ross, P. N. In *Interfacial Electrochemistry: Theory, Experiment, and Applications*; Wieckowski, A., Ed.; Marcel Dekker: New York, 1999; pp 821−841.

(2) *Proceedings of the Symposium on Oxygen Electrochemistry*; Adzic, R. R., Anson, F. C., Kinoshita, K., Eds.; The Electrochemical Society, Inc.: New Jersey, 1996.

(3) Wiesener, K.; Ohms, D. In *Electrochemical Hydrogen Technologies*; Wendt, H., Ed.; Elsevier: Amsterdam, 1990; pp 63−102.

(4) Tarasevich, M. R.; Sadkowski, A.; Yeager, E. In *Comprehensive Treatise of Electrochemistry*; Conway, B. E., et al., Eds.; Plenum: New York, 1983; Vol. 7, pp 301−398.

(5) Jerkiewicz, G. In *Interfacial Electrochemistry: Theory, Experiment, and Applications*; Wieckowski, A., Ed.; Marcel Dekker: New York, 1999; pp 559−576.

(6) Conway, B. E. *Prog. Surf. Sci.* **1995**, *49*, 331−452.

(7) Bard, A. J.; Fan, F.-R. F.; Mirkin, M. V. In *Electroanalytical Chemistry*; Bard, A. J., Ed.; Marcel Dekker: New York, 1994; Vol. 18, pp 243−373.

(8) *Scanning Electrochemical Microscopy*; Bard, A. J., Mirkin, M. V., Eds.; Marcel Dekker: New York, 2001.

(9) Zhou, J.; Zu, Y.; Bard, A. J. *J. Electroanal. Chem.* **2000**, *491*, 22. (b) Jambunathan, K.; Shah, B. C.; Hudson, J. L.; Hillier, A. C. *J. Electroanal. Chem.* **2001**, *500*, 279.

(10) Abdelsalam, M. E.; Denuault, G.; Baldo, M. A.; Bragato, C.; Daniele, S. *Electroanalysis* **2001**, *13*, No. 4.

(11) Daniele, S.; Baldo, M. A.; Bragato, C. *Anal. Chem.* **1999**, *71*, 811−818.

(12) Abdelsalam, M. E.; Denuault, G.; Baldo, M. A.; Bragato, C.; Daniele, S. *J. Electroanal. Chem.* **1998**, *449*, 5.

(13) Kolthoff, I. M.; Lingane, J. J. *Polarography*; Interscience: New York, 1952; p 52.

(14) Hoare, J. P. In *Encyclopedia of Electrochemistry of Elements*; Bard, A. J., Ed.; Marcel Dekker: New York, 1974; Vol. II, pp 191−382.

(15) Gilman, S. In *Electroanalytical Chemistry*; Bard, A. J., Ed.; Marcel Dekker: New York, 1967; Vol. 2, pp 133−146.

(16) Bard, A. J.; Mirkin, M. V.; Unwin, P. R.; Wipf, D. O. *J. Phys. Chem.* **1992**, *96*, 1861.

(17) Mirkin, M. V.; Arca, M.; Bard, A. J. *J. Phys. Chem.* **1993**, *97*, 10790.

(18) Arca, M.; Mirkin, M. V.; Bard, A. J. *J. Phys. Chem.* **1995**, *99*, 5040.

(19) Mirkin, M. V.; Fan, F.-R. F.; Bard, A. J. *J. Electroanal. Chem.* **1992**, *328*, 47.

(20) George, W. H.; Dinius, R. H. *J. Chem. Eng. Data* **1972**, *17*, 449.

(21) Hsueh, K.-L.; Gonzalez, E. R.; Srinivasan, S. *Electrochim. Acta.* **1983**, *28*, 691.

(22) Strebel, K. A.; McLarnon, F. R.; Cairns, E. *J. Electrochem. Soc.* **1990**, *137*, 3351.

(23) Appleby, A. J.; Borucka, A. *J. Electrochem. Soc.* **1969**, *116*, 1212.

(24) *Electrochemical Methods: Fundamentals and Applications*; Faulkner, L. R., Bard, A. J., Eds.; Wiley: New York, 2001; p 103.

(25) *Electrochemical Oxygen Technologies*; Kinoshita, K., Ed.; John Wiley & Sons: New York, 1992; pp 19−112.

(26) Chen, G.; Delafuente, D. A.; Sarangapani, S.; Mallouk, T. E. *Catal. Today* **2001**, *67*, 341.